Supplementary Information

Fluoride-ion-binding promoted photoinduced charge separation in a self-assembled C_{60} alkyl cation bound bis-crown ether-oxoporphyrinogen supramolecule

Whitney A. Webre,[a] Habtom B. Gobeze,[a] Shuai Shao,[a] Paul A. Karr,[b] Katsuhiko Ariga,[c,d]
Jonathan P. Hill,*[,c] and Francis D'Souza*[,a]

[a]Department of Chemistry, University of North Texas, 1155 Union Circle, #305070,
Denton TX 76203-5017 USA. Tel: 940-369-8832.
E-mail: Francis.DSouza@unt.edu
[b]Department of Physical Sciences and Mathematics, Wayne State College, 111 Main Street,
Wayne, Nebraska 68787, USA
[c]Center for Materials Nanoarchitectonics (WPI-MANA), National Institute of Materials
Science (NIMS), Namiki 1-1, Tsukuba, Ibaraki, 305-0044, Japan.
E-mail: Jonathan.Hill@nims.go.jp
[d]Department of Advanced Materials Science, Graduate School of Frontier Sciences, The
University of Tokyo, 5-1-5 Kashiwanoha, Kashiwa, Chiba 277-8561, Japan

Experimental Section

Chemicals. Reagents and dehydrated solvents (in septum-sealed bottles) used for syntheses and spectroscopic measurements were obtained from Tokyo Kasei Chemical Co., Wako Chemical Co. or Aldrich Chemical Co. and were used without further purification. Tetra-n-butylammonium perchlorate, (n-Bu_4N)ClO_4, used in electrochemical studies was from Fluka Chemicals.

Synthesis

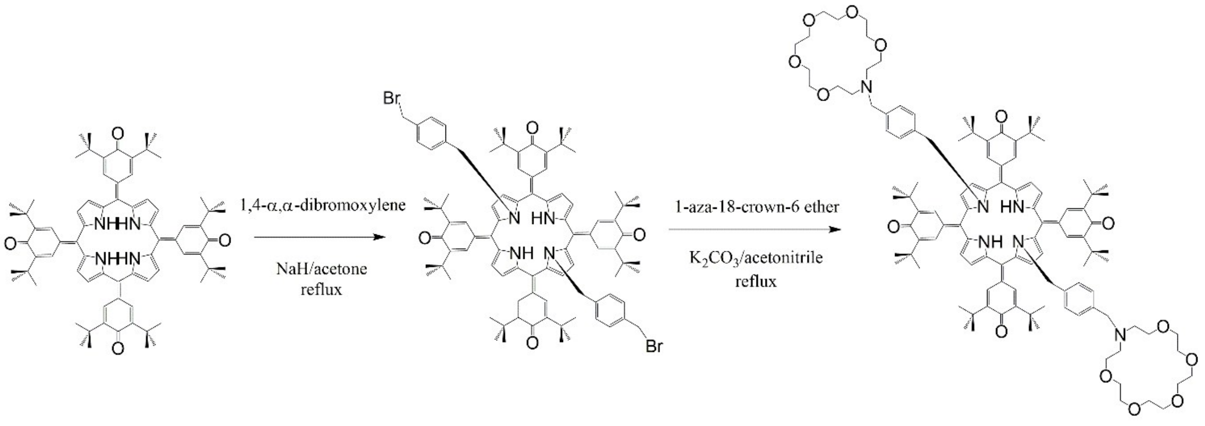

N_{21},N_{23}-Bis(4-bromomethylbenzyl)-5,10,15,20-*tetrakis*(3,5-di-*t*-butyl-4-oxo-cyclohexa-2,5 -dienylidene)porphyrinogen.

5,10,15,20-*tetrakis*(3,5-di-t-butyl-4-hydroxyphenyl)porphyrin (TDtBHPP, 320 mg, 2.84×10^{-4} mol) was dissolved in acetone (35 mL) then sodium hydride (100 mg, 60% suspension in mineral oil) was added.[S1] The reaction was refluxed with stirring under air for 20 m. α,α-(Dibromo)-*p*-xylene (300 mg, 1.14×10^{-3} mol, 4 eq) was then added and the reaction was refluxed for 30 m. A further aliquot of α,α-(dibromo)-*p*-xylene (200 mg, 7.6×10^{-4} mol) was added and the reaction further refluxed for 90 m whereafter a further aliquot of α,α-(dibromo)-*p*-xylene (200 mg, 7.6×10^{-4} mol) was added. Reflux was continued for a further 3 h with monitoring using thin layer chromatography (SiO_2, CH_2Cl_2). The reaction was then allowed to cool and the solvents were removed under reduced pressure. The residue was subjected to column chromatography on silica gel with gradient elution using dichloromethane:hexane (60:40→80:20→100 % CH_2Cl_2) with the product being eluted at 100 % CH_2Cl_2. Product containing fractions were combined and the solvents removed under reduced pressure giving a green solid which was used in the next step without further purification. Yield: 120 mg (28 %). ^{1}H-NMR ($CDCl_3$/THF-d_8 (2:1 v/v), 300 MHz, 298 K): δ = 1.24 (s, 36H, tBu-H), 1.35 (s, 36H, tBu-H), 4.34 (s, 4H, -CH_2Br), 4.53 (s, 4H, -CH_2N), 6.59 (s, 4H, (NH)pyrrole-β-H), 6.63 (d, J = 7.8 Hz, 4H, xylyl-H), 6.93 (d, J = 1.8 Hz, 4H, pyrrole-β-H), 7.21 (d, J = 1.8 Hz, 4H, cyclohexadienylidene-H), 7.16 (d, J = 7.8 Hz, 4H, xylyl-H), 7.62 (d, J = 2.4 Hz, 4H, cyclohexadienylidene-H), 10.27 (s, 2H, NH) ppm. FTIR (KBr pellet): ν = 2999.1 (w, Ar C-H(str.)); 2955.9, 2919.1, 2864.5 (all m, C-H(str.); 1596.8 (s, C=O(str.)); 1533.1 (w, C=C(str.)); 1488.3, 1464.7 (m, C=C, C=N (str.)); 1388.3 (w); 1361.3 (s); 1331.6 (m); 1317.2 (m); 1298.2(m); 1261.3 (m); 1229.9 (w); 1204.7 (w); 1089.1 (m); 1029.1 (m); 948.1 (m); 929.7 (w); 886.7 (w); 841.2 (w); 819.4 (w); 809.6 (w); 743.4 (w); 628.1 (w); 531.9 (w) cm^{-1}. MALDI-TOF-MS (dithranol): calc'd for $C_{92}H_{104}Br_2N_4O_4$ 1488.67, found 1486.48 ([M – 2H]$^+$). This compound gradually precipitates from samples prepared for NMR precluding measurement of its ^{13}C NMR spectrum.

N$_{21}$,N$_{23}$-Bis(1-aza-18-crown-6-methylbenzyl)-5,10,15,20-*tetrakis*(3,5-di-*t*-butyl-4-oxo-cyclohexa-2,5-dienylidene)porphyrinogen.

N$_{21}$,N$_{23}$-Bis(4-bromomethylbenzyl)-5,10,15,20-*tetrakis*(3,5-di-*t*-butyl-4-oxo-cyclohexa-2,5-dienylidene)porphyrinogen (50 mg, 3.35×10^{-5} mol) was dissolved in acetonitrile (10 mL) then 1-aza-18-crown-6 ether (50 mg, ~2.5 eq) dissolved in acetonitrile (5 mL) was added. Potassium carbonate (100 mg) was then added and the resulting mixture refluxed overnight (18 h). The reaction was then cooled poured into water (20 mL) and extracted with dichloromethane (20 mL × 2). The organic extracts were combined, dried over anhydrous sodium sulfate followed by filtration and removal of solvents under reduced pressure. The resulting green solid was purified by gel permeation chromatography using BioBeads SX-1 eluting with dichloromethane. Product-containing fractions were combined and solvents evaporated yielding a green solid. The sample could be further purified by recrystallization from dichloromethane/acetone. Yield: 56 mg (89 %). ^{1}H-NMR ($CDCl_3$, 300 MHz, 298 K) δ = 1.24 (s, 36H, tBu-H), 1.34 (s, 36H, tBu-H), 2.65 (t, 8H, N-(CH_2)$_2$), 3.64 – 3.49 (m, 44H, crown O-(CH_2), Ph-(CH_2)-N)), 4.50 (s, 4H, benzylic-CH_2), 6.52 (d, J = 1.1 Hz, 4H, pyrrole-β-H), 6.68 (d, J = 7.32 Hz, 4H, benzyl-Ar-H), 6.90 (s, 4H, pyrrole-β-H), 7.05 (s, 4H), 7.09 (d, J = 7.32 Hz, 4H, benzyl-Ar-H), 7.58 (s, 4H), 10.30 (s, 2H, NH) ppm. ^{13}C-NMR ($CDCl_3$, 75 MHz, 298 K) δ = 29.46, 35.27, 35.55, 49.05, 53.53, 59.25, 69.79, 70.24, 70.65, 70.75, 119.24, 120.11, 126.77, 128.99, 131.25, 131.51, 132.07, 135.22, 135.54, 136.84, 139.78, 146.89, 147.95, 185.93 ppm. FTIR (KBr pellet): ν = 2999.7 w, Ar C-H(str.); 2964.8, 2918.6, 2866.2 (all m, C-H(str.); 1592.9 (s, C=O(str.)); 1561.9 (w, C=C(str.)); 1530.1 (w, C=C(str.)); 1488.3 (m); 1466.1 (m); 1412.2 (w); 1405.1 (w); 1387.7 (w); 1360.6 (s); 1315.4 (m); 1261.2 (m); 1205.2 (w); 1120.9 (m); 1089.4 (m); 1042.4 (w); 1028.5 (m); 1005.5 (w); 986.0 (w); 949.6 (m); 929.3 (w); 886.8 (w); 840.8 (w); 819.2 (w); 807.9 (w0; 746.3 (w); 830.7 (w); 533.3 (w); 518.9 (w) cm^{-1}. MALDI-TOF-MS (dithranol): calc'd for $C_{116}H_{154}N_6O_{14}$ 1855.15, found 1855.18 ([M]$^+$).

The synthesis of C_{60} alkyl ammonium cation is given elsewhere.[S2]

Spectral measurements: ^{1}H-NMR spectra were obtained using a JEOL AL300BX spectrometer using tetramethylsilane as an internal standard. MALDI-TOF mass spectra were measured using a Shimadzu Axima AFR+ mass spectrometer with dithranol as matrix.

The UV-visible spectral measurements were carried out with a Shimadzu Model 2550 double monochromator UV-visible spectrophotometer. The fluorescence emission was monitored by using a Horiba Yvon Nanolog coupled with time-correlated single photon counting with nanoLED excitation sources. A right angle detection method was used. Differential pulse voltammograms were recorded on an EG&G PARSTAT electrochemical analyzer using a three electrode system. A platinum button electrode was used as the working electrode. A platinum wire served as the counter electrode and an Ag/AgCl electrode was used as the reference electrode. Ferrocene/ferrocenium redox couple was used as an internal standard. All the solutions were purged prior to electrochemical and spectral measurements using nitrogen gas.

Femtosecond pump-probe transient spectroscopy: Femtosecond transient absorption spectroscopy experiments were performed using an Ultrafast Femtosecond Laser Source (Libra) by Coherent incorporating diode-pumped, mode locked Ti:Sapphire laser (Vitesse) and diode-pumped intra cavity doubled Nd:YLF laser (Evolution) to generate a compressed laser output of 1.45 W. For optical detection, a Helios transient absorption spectrometer coupled with femtosecond harmonics generator both provided by Ultrafast Systems LLC was used. The source for the pump and probe pulses were derived from the fundamental output of Libra (Compressed output 1.45 W, pulse width 100 fs) at a repetition rate of 1 kHz. 95% of the fundamental output of the laser was introduced into a TOPAS-Prime-OPA system with 290-2600 nm tuning range from Altos Photonics Inc., (Bozeman, MT), while the rest of the output was used for generation of white light continuum. Kinetic traces at appropriate wavelengths were assembled from the time-resolved spectral data. Data analysis was performed using Surface Xplorer software supplied by Ultrafast Systems. All measurements were conducted in degassed solutions at 298 K. The estimated error in the reported rate constants is $\pm$10%.

References

S1. E. Dolušić, S. Toppet, S. Smeets, L. V. Meervelt, B. Tinant and W. Dehaen, *Tetrahedron*, 2003, **59**, 395–400.

S2. F. D'Souza, R. Chitta, S. Gadde, D.-M. S. Islam, A. L. Schumacher, M. E. Zandler, Y. Araki and O. Ito, *J. Phys. Chem. B* 2006, **110**, 25240.

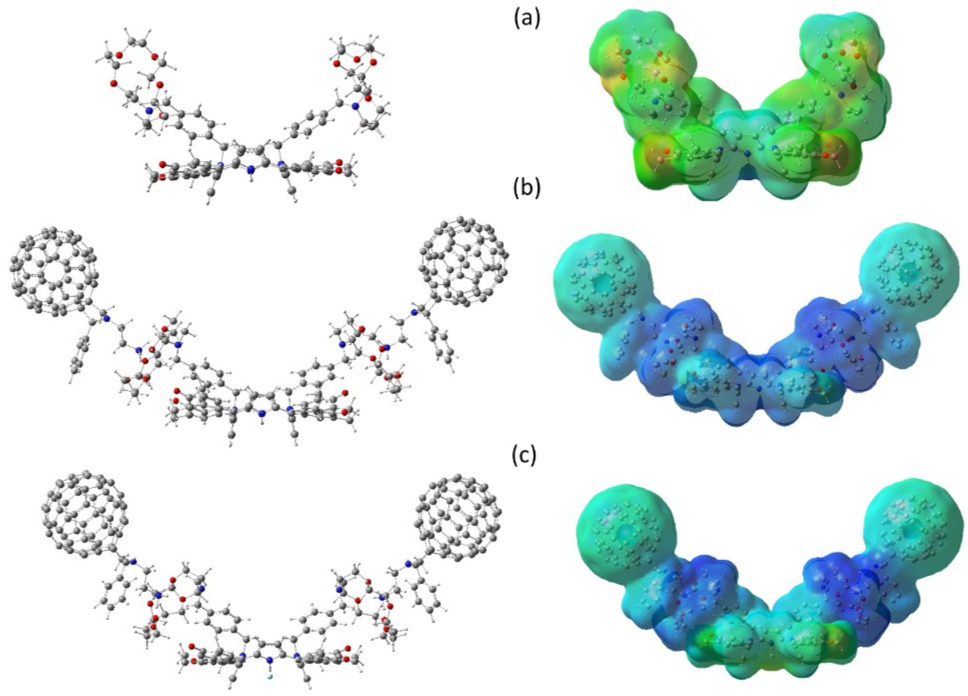

Fig. S1. B3LYP/6-31G** optimized geometry and MEP maps of (a) OxP(Crown)$_2$, (b) OxP(Crown:C$_{60}$)$_2$, and (c) F$^-$:OxP(Crown:C$_{60}$)$_2$.

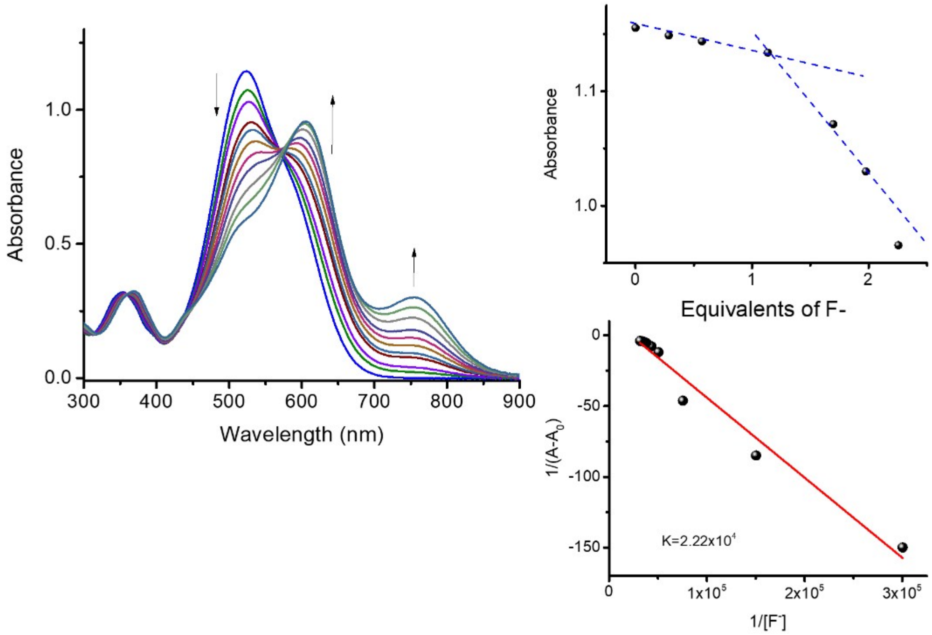

Fig. S2. (a) Absorption spectra of OxP(Crown)$_2$ (1.5 x 10^{-5} M, black trace) upon increasing addition of F$^–$ (0.002 M total addition) in *o*-dichlorobenzene. (b) mole ratio plot to obtain the F$^-$ binding stoichiometry of the F$^-$:OxP(Crown)$_2$ complex, (c) Benesi-Hildebrand plot constructed to obtain F$^-$ binding constant.

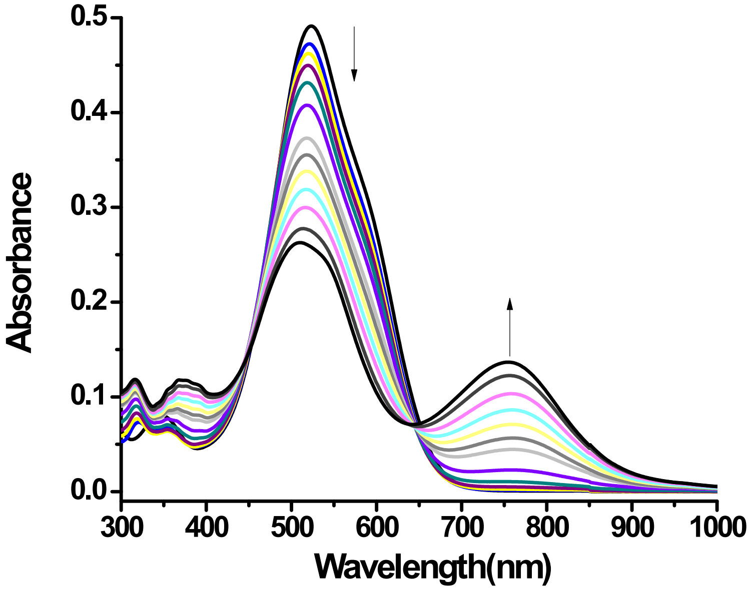

Fig. S3. Spectral changes observed during oxidation of OxP(Crown)$_2$ in benzonitrile. Nitrosonium tetrafluoroborate was used as an oxidizing agent.

Spectra of N$_{21}$,N$_{23}$-Bis(1-aza-18-crown-6-methylbenzyl)-5,10,15,20-*tetrakis*(3,5-di-*t*-butyl-4-oxo-cyclohexa-2,5-dienylidene)porphyrinogen

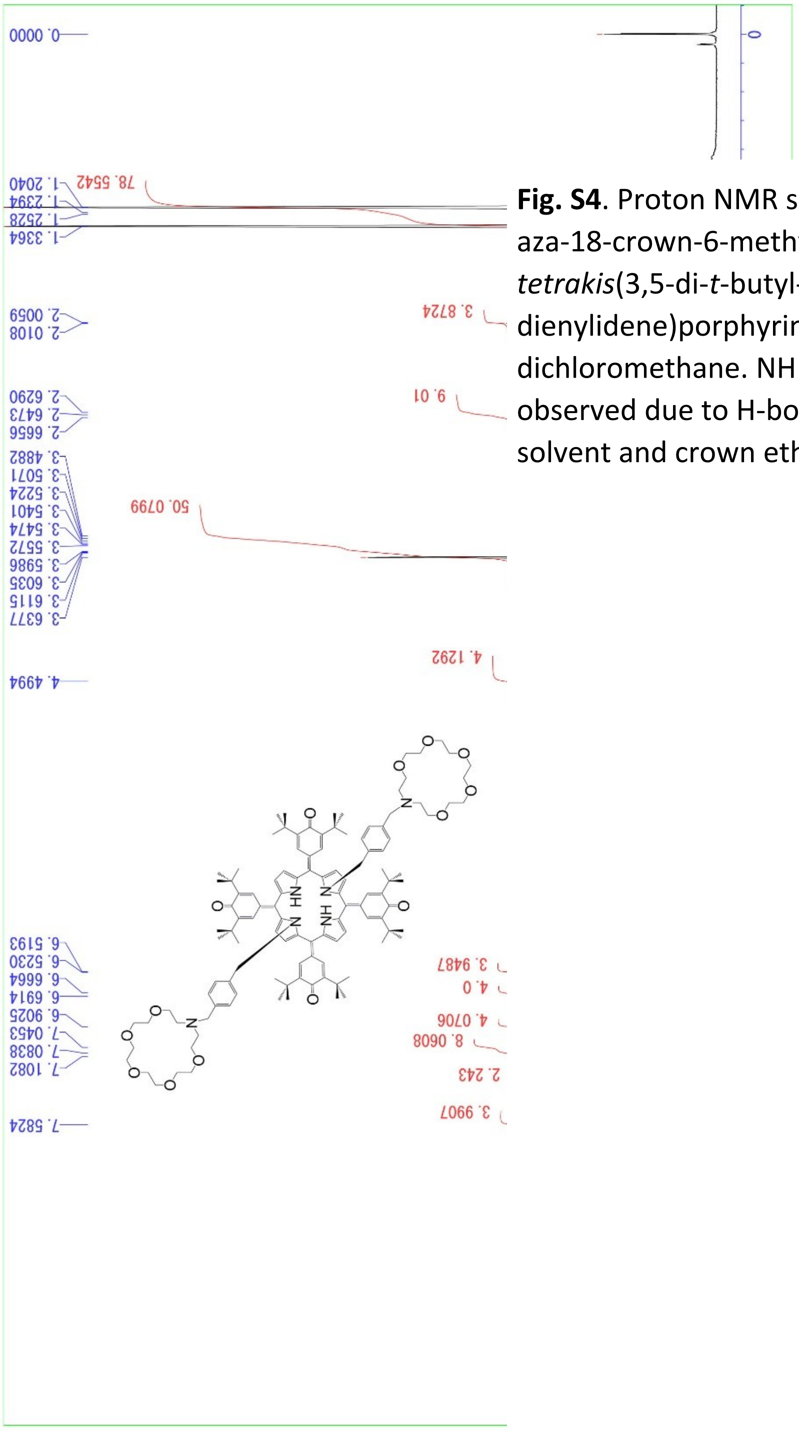

Fig. S4. Proton NMR spectrum of N$_{21}$,N$_{23}$-Bis(1-aza-18-crown-6-methylbenzyl)-5,10,15,20-*tetrakis*(3,5-di-*t*-butyl-4-oxo-cyclohexa-2,5-dienylidene)porphyrinogen. Asterisk denotes dichloromethane. NH groups could not be observed due to H-bonding interactions with solvent and crown ether moieties.

Fig. S5. ^{13}C NMR spectrum of N_{21},N_{23}-Bis(1-aza-18-crown-6-methylbenzyl)-5,10,15,20-*tetrakis*(3,5-di-*t*-butyl-4-oxo-cyclohexa-2,5-dienylidene)porphyrinogen.

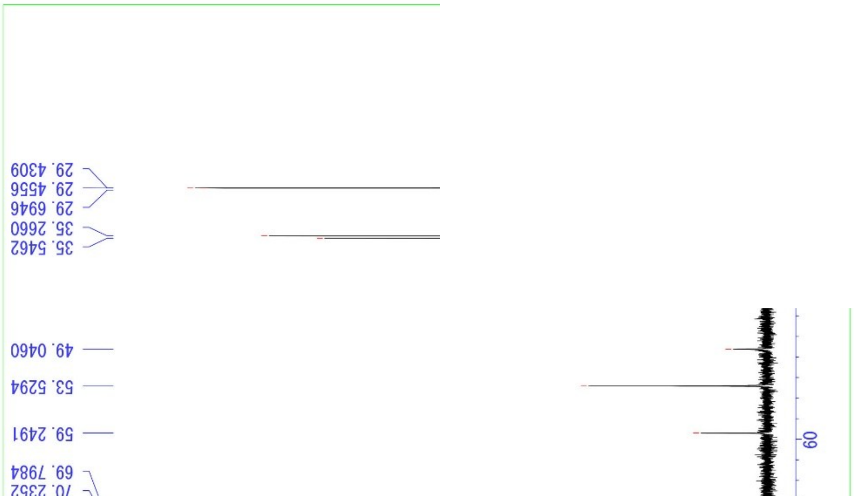

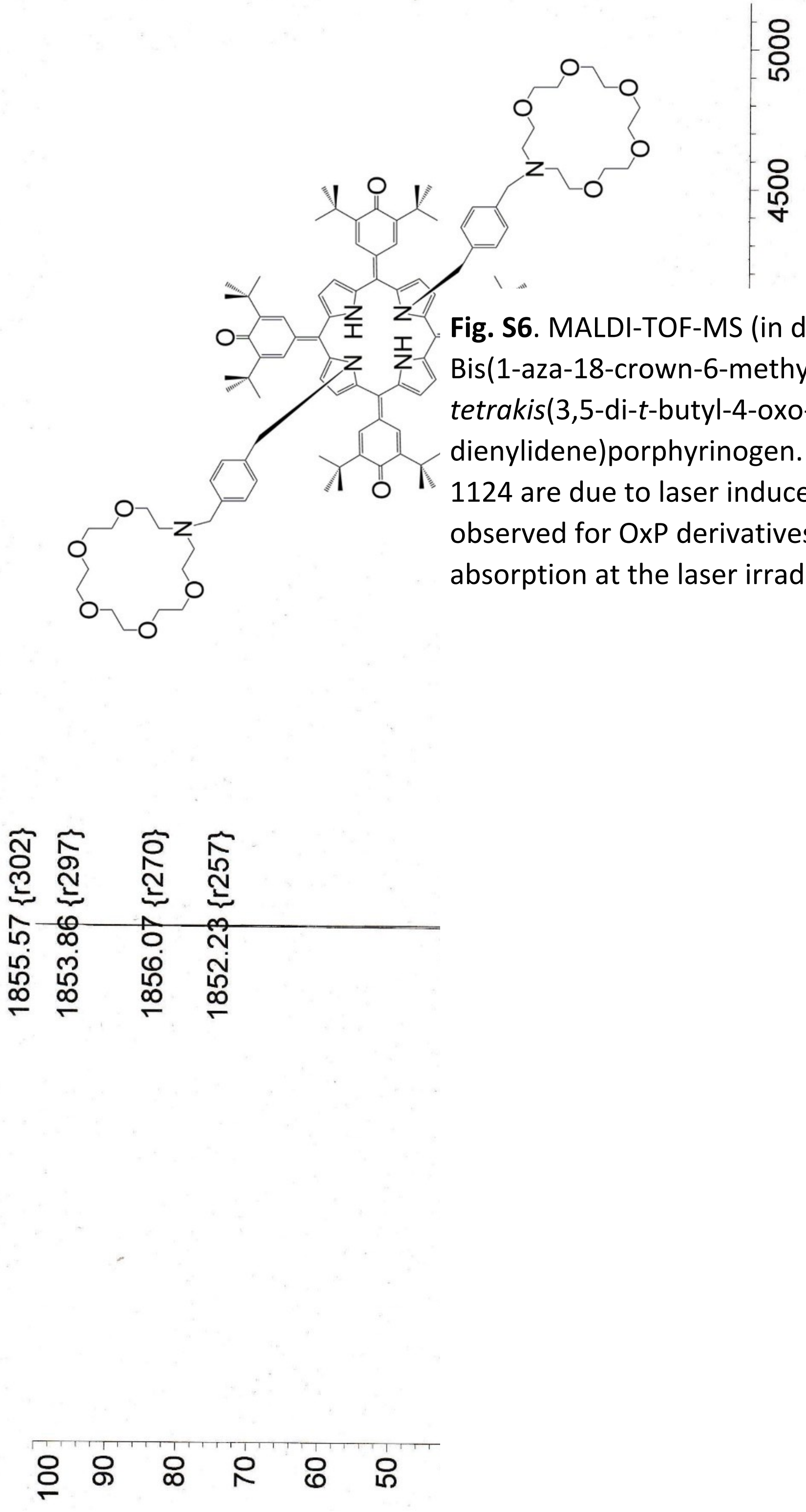

Fig. S6. MALDI-TOF-MS (in dithranol) spectrum of N_{21},N_{23}-Bis(1-aza-18-crown-6-methylbenzyl)-5,10,15,20-*tetrakis*(3,5-di-*t*-butyl-4-oxo-cyclohexa-2,5-dienylidene)porphyrinogen. Additional peaks at m/z 1490, 1124 are due to laser induced dealkylation commonly observed for OxP derivatives probably due to strong absorption at the laser irradiation wavelength.

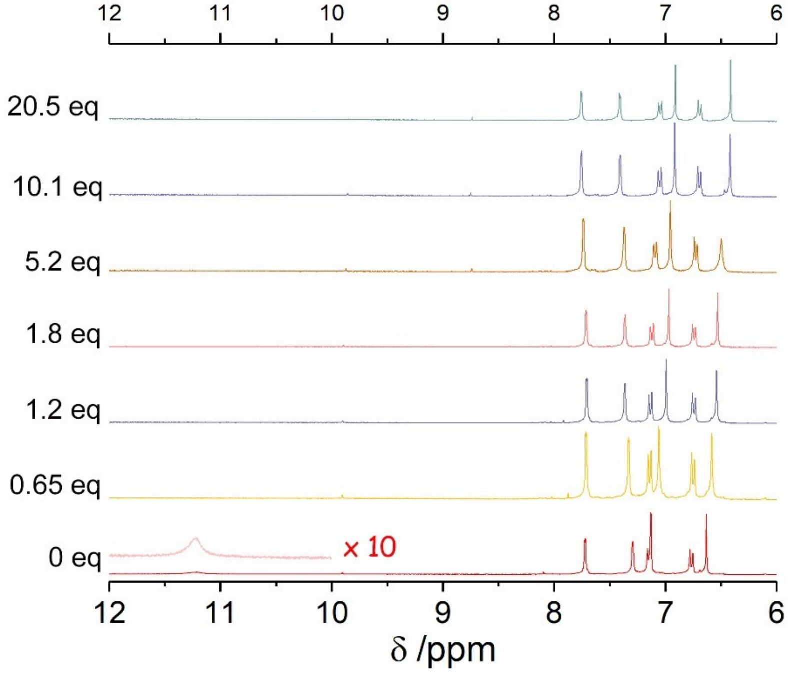

Fig. S7. Low field region of ^{1}H NMR spectra of OxP(Crown)$_2$ in the presence of increasing quantities of tetra-*n*-butylammonium fluoride in acetone-d_6. NH resonance at 11.2 ppm cannot be observed in the presence of fluoride anions due to guest exchange.

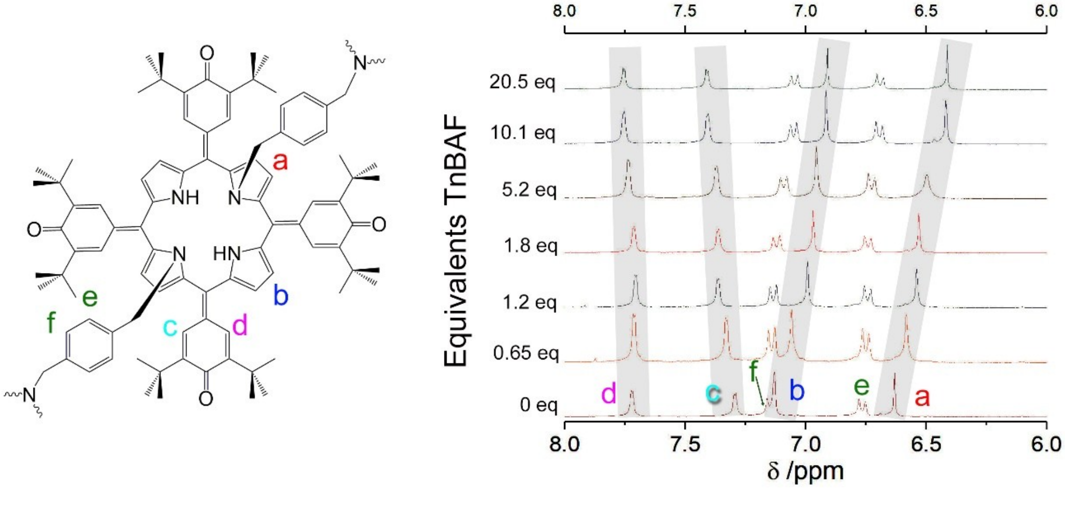

Fig. S8. Assignment of ^{1}H NMR spectra of OxP(Crown)$_2$. Pyrrole β-H resonances at 6.6 and 7.1 ppm are gradually shifted upfield with increasing quantities of fluoride anions. Meso-substituents are hardly affected supporting the H-bonding of F$^-$ at the pyrrole NH groups.

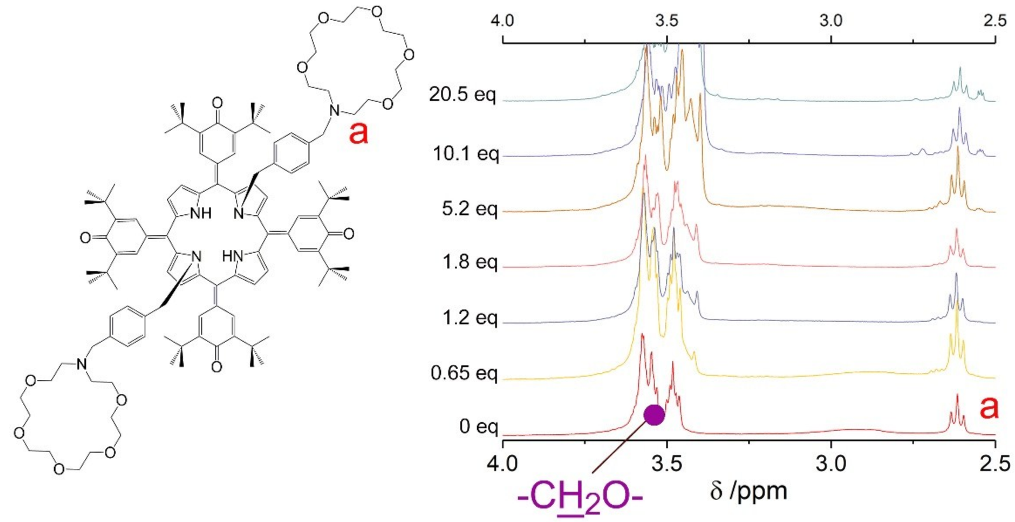

Fig. S9. ^{1}H NMR spectra of OxP(Crown)$_2$ (crown ether peaks) in the presence of increasing quantities of tetra-*n*-butylammonium fluoride in acetone-d_6 revealing a lack of any interaction at the aza-crown substituents.

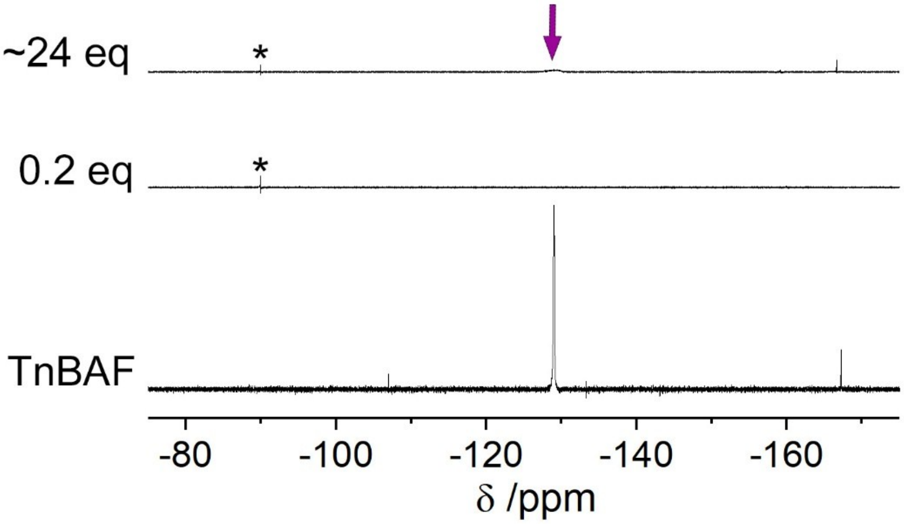

Fig. S10. ^{19}F NMR spectrum of tetra-*n*-butylammonium fluoride in acetone-d_6 (lower). The upper spectra are ^{19}F NMR spectra of OxP(Crown)$_2$ in the presence of the indicated quantities of tetra-*n*-butylammonium fluoride. Fluoride could not be detected except in the presence of large quantities over 20 eq TnBAF. The peak around 168 ppm is due to a fluorine containing contaminant, probably bifluoride. Asterisk denotes an instrumental artefact.